Design and Application of a Nested Multi-Channel Sodium/Proton Knee Array at 3T

Ryan Brown[1], Karthik Lakshmanan[1], Guillaume Madelin[1], Gregory Chang[1], Daniel K Sodickson[1], Ravinder R Regatte[1], and Graham C Wiggins[1]
[1] *The Bernard and Irene Schwartz Center for Biomedical Imaging, Dept. of Radiology, New York University School of Medicine, New York, NY, United States*

INTRODUCTION: Sodium MRI has shown promise for glycosaminoglycan assessment in knee cartilage with the potential for early osteoarthritis detection (1). One of the fundamental challenges in sodium MRI is the relatively low sensitivity due to low sodium concentration in the cartilage and low receptivity. Multi-channel phased array coils have helped alleviate this limitation at 7T, enabling 2 mm isotropic knee imaging in 13min (2). In this work, we describe a 3T 6 channel dual-nuclei knee coil whose design counteracts low coil-tissue coupling by implementing a wideband matching scheme and a mechanically flexible former.

METHODS: ***Sodium Receive Array:*** Two key elements distinguish the proposed 3T dual-nuclei sodium/proton knee coil from conventional knee coils:

1) A mechanically flexible sodium receive array was implemented to minimize the coil-tissue distance and reduce the allowable former diameter (Fig. 1). Whereas rigid knee coils typically require ~20cm diameter to accommodate a range of patient sizes, the proposed flexible coil was reduced to 15cm diameter without compromising accessibility. The flexible inner shell is discontinuous between coils 1 and 6, allowing the array be wrapped around the knee. This helped counteract the low coil-tissue coupling that is characteristic of coils operating at a low resonance frequency (in this case 32.6 MHz). The coil count of six [7.9cm (arc length) × 15cm (head/foot)] was selected empirically based on target unloaded-to-loaded Q-factor ratio of two and desired head/foot coverage of roughly 12cm.

2) Despite the coils' close proximity to the tissue, low coil-tissue coupling resulted in a relatively high loaded Q-factor. This intensifies SNR degradation due to preamplifier noise coupling, which scales with kQ, where k is the normalized magnetic coupling and can be substantial for next nearest neighbor coils (3-4). This additional noise appears on the diagonal elements of the correlation matrix and therefore cannot be counteracted in image reconstruction. To mitigate this effect, wideband matching was applied by introducing an impedance mismatch at the coil port. The optimal wideband match condition was calculated using $|S_{11}|=[|1+ikQ|*Z_0-Z_0|/[|1+ikQ|*Z_0+Z_0]$, where the magnetic coupling factor (f_0/f_{split}) was k=0.12 for the gapped coils (Ch1 & Ch6) and k=0.03 for other next nearest neighbors, Z_0=50Ω, and Q_{loaded}≈100. Correspondingly, coils 1 and 6 were matched to $|S_{11}|$=0.86 and coils 2 to 5 were matched to $|S_{11}|$=0.49. For comparison, SNR was measured in a phantom with the array matched using both the wideband scheme and the conventional scheme where $|S_{11}|$=0.

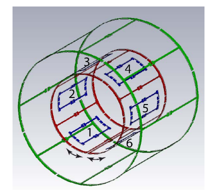

Fig. 1. A flexible inner shell houses the 6ch sodium receive array (red) and 6ch proton transceiver array (blue). A rigid outer shell houses the sodium birdcage (green).

Detunable Sodium Birdcage: A high pass sodium birdcage coil was preferred for sodium transmit because its non-uniform high-order modes occur at frequencies well below the proton resonant frequency. Simulations similar to those previously described were used to guide the choice of birdcage dimensions (25cm diameter × 15cm length) (2,5).

Proton Transmit-Receive Array: An array of six proton coils was constructed to provide adequate SNR in the knee articular cartilage with minimal disturbance to the sodium channel. The sodium receive coils exhibit low impedance at the proton frequency and therefore act as a shield. To avoid shielding the proton elements while simultaneously minimizing coil-tissue distance, the proton coils were arranged concentric to the sodium coils and also shared the same former (Fig. 1). The coils were driven through Wilkinson dividers such that equal power and a fixed phase offset of 60° was realized between adjacent elements. Dimensions of 3.2cm (arc length) × 10cm (head/foot) were empirically selected based on tradeoffs between coverage and uniformity of large coils and tolerable coil coupling offered by small coils.

Imaging: Phantom and *in vivo* knee joint measurements were performed using a whole-body 3T scanner (TIM Trio, Siemens) upon approval by our local IRB and informed written consent from the participants. The dual-nuclei array was compared to two mono-nuclear coils (sodium: birdcage transceiver coil, 20cm diameter and 17cm length; proton: birdcage transmit, 15ch receive array (approx 18cm diameter × 20cm length, QED) via measurements in the same phantom or participant.

RESULTS: ***Sodium:*** The wideband matched sodium array provided a posterior SNR gain of roughly 20-50% over the conventionally matched array primarily by counteracting strong coupling between coils 1 and 6 (arrow, Fig. 2) and minor 10% gain in the center. Further, the flexible receive array's reduced diameter provided a 30% SNR gain over the mono-nuclear sodium birdcage in the center and >2-fold in the periphery, which is the location of the patella articular cartilage. Sodium imaging using a custom FLORET (6) sequence (4mm isotropic resolution, 8.5mins) showed similar qualitative advantages (Fig 2). Sodium B1+ uniformity (mean/standard deviation flip angle) was 96% in the central transverse slice with the proposed coil, while a 180° excitation with a 1ms hard pulse required 200v for both the constructed coil and the mono-nuclear birdcage.

Proton: Due to the sparsely arranged proton coils in the dual-nuclei array, central SNR was roughly 67% that of the 15ch mono-nuclear array (Fig. 3). The sparse local coils expectedly caused local B1+ hot spots in the posterior knee, though the central transmit uniformity was adequate for PDw FSE imaging (Fig. 3). The head-foot coverage (FWHM) and 90° transmit voltage were 6.7cm and 129v (dual-nuclei array) and 15.5cm and 117v (mono-nuclear array), respectively.

DISCUSSION: At frequencies as low as 32.6 MHz tissue losses are small and the resulting low unloaded to loaded Q ratio can make the potential gains from a phased array difficult to realize. This issue was addressed here by using a mechanically flexible former to minimize coil to tissue distance and reduce the overall diameter of the array and by implementing a wideband matching scheme. The resulting dual-nuclei array provided substantial SNR gain in articular cartilage regions compared to a mono-nuclear sodium birdcage coil. Further, the wideband matching scheme provided additional gain over the conventionally matched sodium array, where preamplifier noise coupling is accentuated due to coil coupling and a characteristically high loaded Q-factor. It is anticipated that this design principle will become increasingly valuable as many-element arrays applied to low gamma nuclei become more prevalent. Note that the broadband match calculations were simplified to that of a two coil array wherein a given coil is assumed to be coupled to only one other coil. A complete eigenmode analysis may produce more favorable match conditions. On the proton channel, central SNR was expectedly lower than the 15ch receive array but 15% better than a mono-nuclear knee birdcage (data not included), suggesting that the proposed design is more favorable than standard "trap-based" dual-nuclei coils where the efficiency of the high-frequency channel is sacrificed. Finally, the gapped proton design resulted in compromised transmit uniformity, which was considered a reasonable trade-off given the sodium SNR priority and the desire to avoid shielding the proton coils from the tissue by the low-impedance sodium coils. We also note that proton uniformity may be further compromised due to non-optimal phase offsets when the former is flexed.

REFERENCES: 1. Reddy R, et al. MRM 1998. 2. Brown R, et al. MRM 2013. 3. Vester M, et al. ISMRM 2012. 4. Wiggins GC, et al. ISMRM 2012. 5. Lattanzi R, et al. NMR Biomed 2010. 6. Pipe J, et al. MRM 2011.

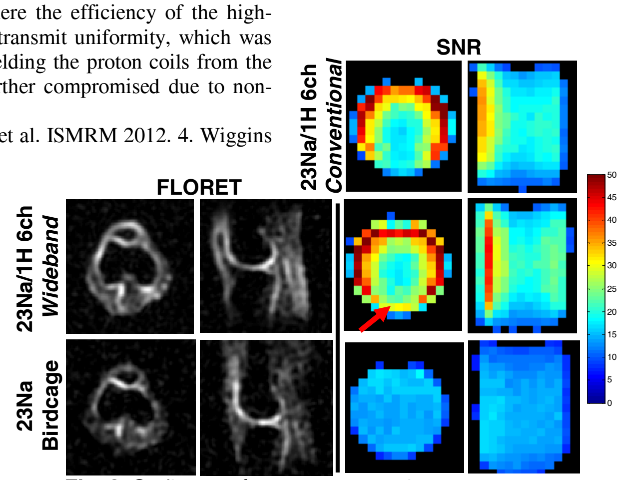

Fig. 2. Sodium performance comparison.

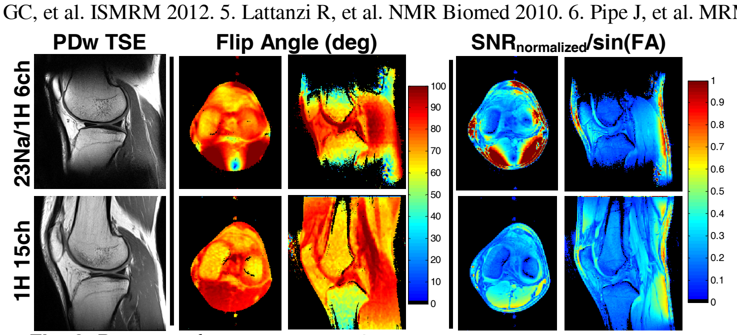

Fig. 3. Proton performance comparison.